Science Advances

AAAS

advances.sciencemag.org/cgi/content/full/4/5/eaar4536/DC1

Supplementary Materials for

Endocytosis-mediated siderophore uptake as a strategy for Fe acquisition in diatoms

Elena Kazamia, Robert Sutak, Javier Paz-Yepes, Richard G. Dorrell, Fabio Rocha Jimenez Vieira, Jan Mach, Joe Morrissey, Sébastien Leon, France Lam, Eric Pelletier, Jean-Michel Camadro, Chris Bowler, Emmanuel Lesuisse

Published 16 May 2018, *Sci. Adv.* **4**, eaar4536 (2018)
DOI: 10.1126/sciadv.aar4536

The PDF file includes:

Other Supplementary Material for this manuscript includes the following:
(available at advances.sciencemag.org/cgi/content/full/4/5/eaar4536/DC1)

- movie S1 (.mov format). Live cell imaging of the uptake of NBD conjugate of FOB (FOB-NBD) by *P. tricornutum*.
- table S1 (Microsoft Excel format). Data used to construct Fig. 6 and fig. S8.

Supplementary figures

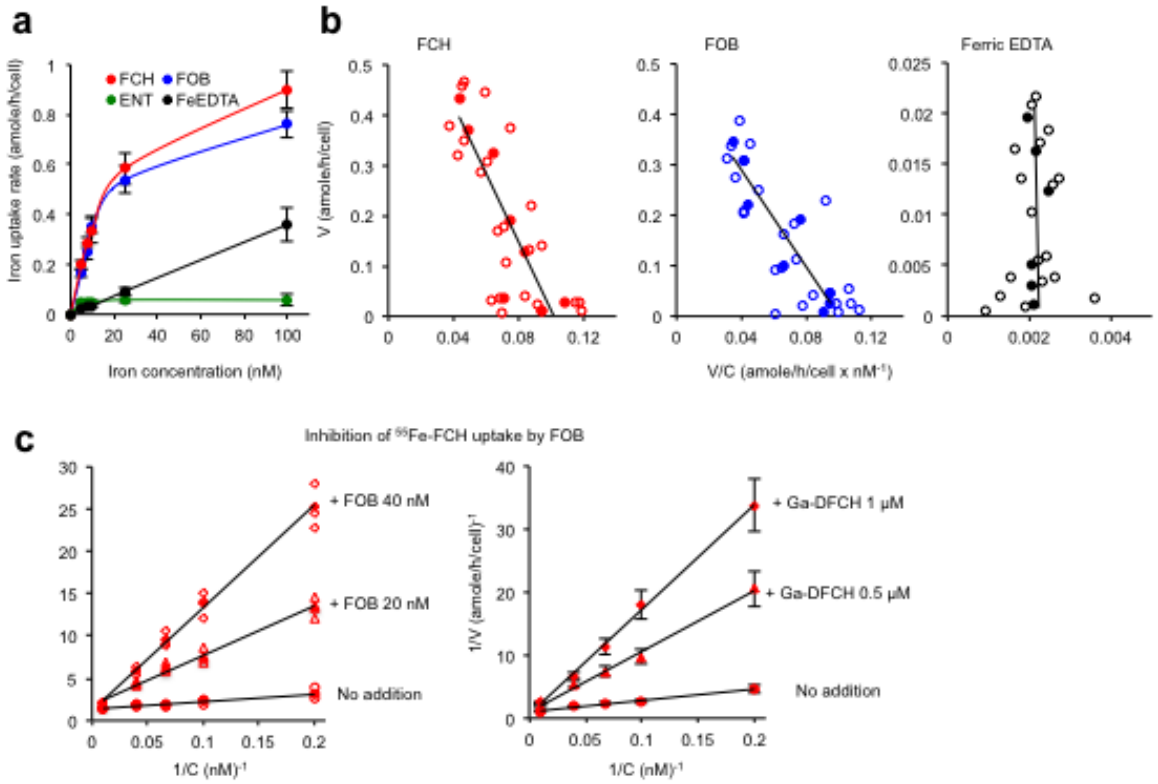

fig. S1. Siderophore uptake in *P. tricornutum* fits simple Michaelis-Menten kinetics. **Panel a:** Iron uptake by wild-type *P. tricornutum* cells follows simple Michaelis-Menten kinetics, indicated by the observation that ^{55}Fe uptake from FCH (red circles) and FOB (blue circles) shows clear saturation with increasing iron concentration, while iron uptake rate from ferric EDTA (black circles) shows no apparent saturation, and ENT uptake (green circles) remains very low in the range of concentrations used. **Panel b:** Eadie-Hofstee representations of iron uptake kinetics from FCH (red) FOB (blue) and ferric EDTA (black), with iron concentration ranging from 0.1 nM to 10 nM. We estimate K_M and Vmax values of 5-7 nM and 0.5-0.7 pmole/h/million cells for FOB and FCH uptake by wild-type cells. We obtained the following equations by linear regression (calculated with the mean values of Eadie-Hofstee plots): FCH uptake: y = -6.5x + 0.6867; FOB uptake: y = -4.8x + 0.4823. **Panel c:** Lineweaver-Burk representation for ^{55}Fe-FCH uptake by wild-type cells, showing competitive inhibition by cold FOB (red triangles: 20 nM; red diamonds: 40 nM) and by the gallium analog of FCH (Ga-DFCH) (red triangles: 0.5 µM; red diamonds: 1 µM). Both acted as competitive inhibitors for ^{55}Fe-FCH uptake with calculated Ki values of 3-5 nM.

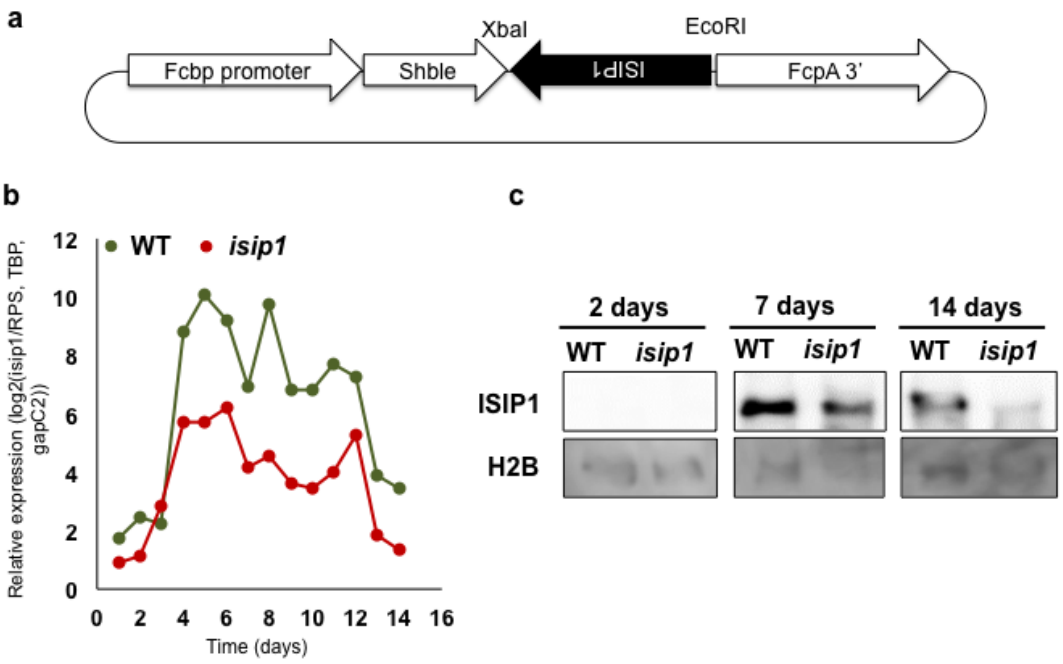

fig. S2. Construction of an *ISIP1* knockdown in *P. tricornutum* and expression of *ISIP1* transcript and protein. *P. tricornutum* was transformed with a vector containing an ISIP1 antisense cassette (**panel a**). To generate this vector ISIP1 was amplified from gDNA adding EcoRI and XbaI sites, then it was cloned into antisense position behind a high expression promoter. ISIP1 gene expression (assessed by quantitative RT-PCR; **panel b**) and protein content (assessed by western blot; **panel c**) are strongly induced after 4 days of iron deprivation to reach a maximum after several days of iron depletion. Abundance of ISIP1 transcript (**panel b**) and protein (**panel c**) were decreased by 20-100 fold in the ISIP1 knockdown lines. In **panel b**, transcript levels were normalized to RPS, TBP and gapC2 transcripts; in c, histone H2B was used as loading control.

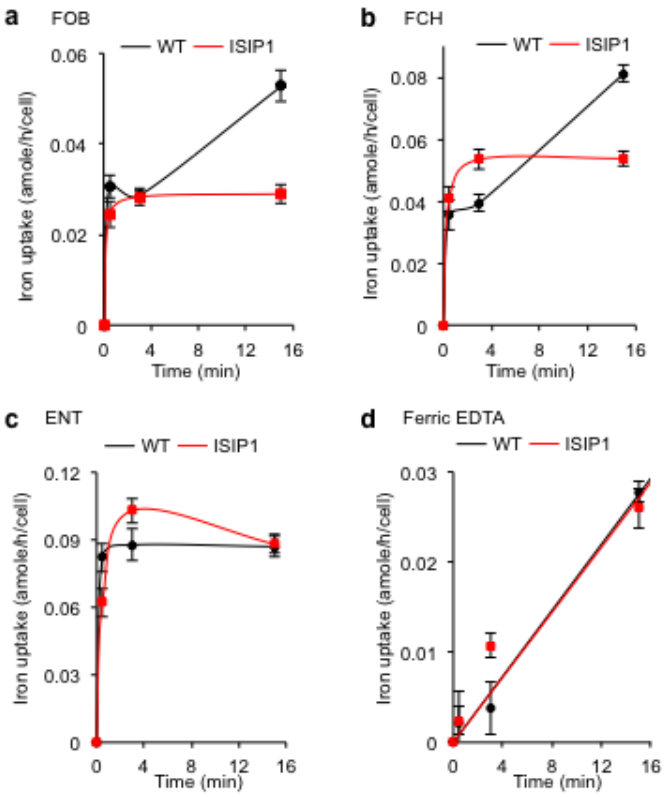

fig. S3. Siderophore uptake involves a binding step. The figure shows short-term iron uptake kinetics from ferrioxamine B (FOB; panel **a**), ferrichrome (FCH; **b**), enterobactin (ENT; **c**) and ferric EDTA (**d**) by *P. tricornutum* (wild-type cells: black; *ISIP1* knockdown cells: red): Cells were grown for one week in iron-deficient medium and washed once prior to the experiment. The cells were then incubated in the wells of a 96-well microtiter plate at about 5x 10^7 cells/ml in growth medium containing 1 µM of ^{55}Fe-labelled FOB (**a**), FCH (**b**), ENT (**c**) or ferric EDTA (**d**). The cells were washed on filters at intervals with the washing buffer, and ^{55}Fe associated to the washed cells was counted by scintillation after bleaching with hypochlorite. Data are means ± SD from 4 experiments (biological replicates).
Siderophores interacted with the cells in 2 steps: a rapid binding step followed by an uptake step. Note that while ENT bound to the cells, it was not taken up and used by the cells. The binding step, unlike uptake, was unaffected in *ISIP1* knockdown cells compared to wild-type cells. This rapid binding step did not occur with ferric EDTA; in this case iron uptake fitted with a linear function of time.

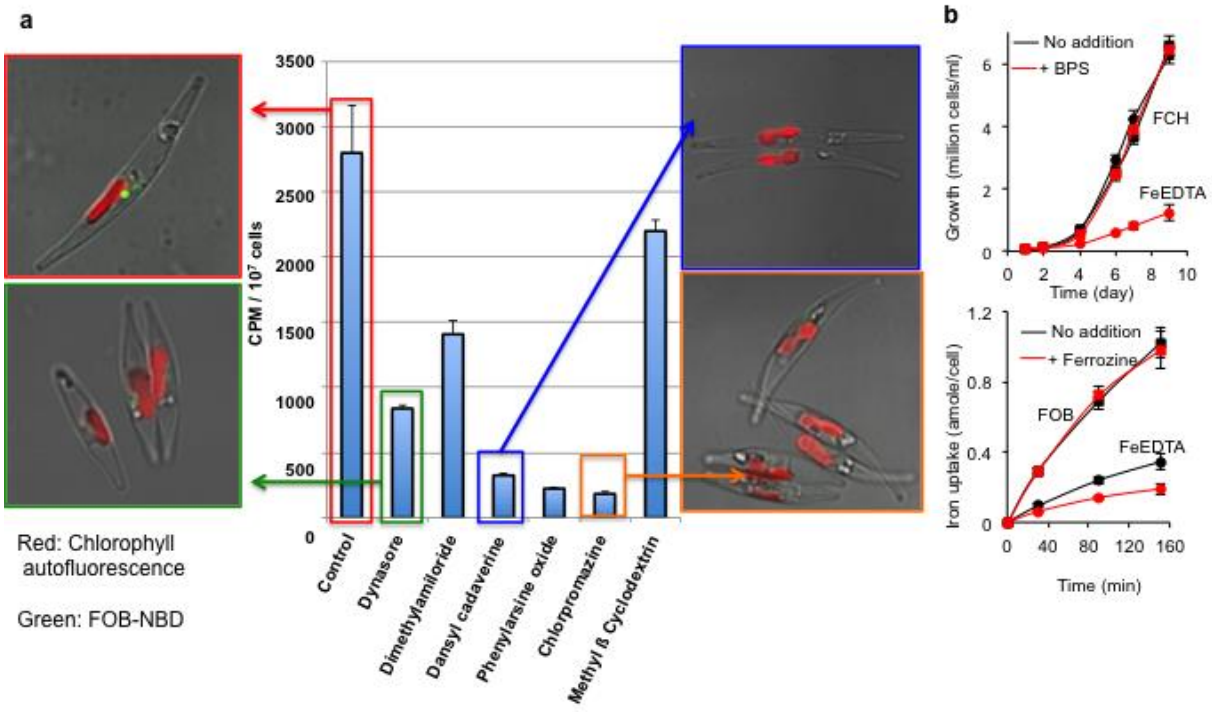

fig. S4. Siderophore uptake involves endocytosis. Panel a: Wild-type cells were grown for 5 days in iron-deficient medium, and then the fluorescent conjugate of desferrioxamine B complexed with gallium (Ga-DFOB-NBD) was added at a final concentration of 1 µM and the endocytosis inhibitors were added at the concentrations indicated in Methods. Microscopy was performed after an overnight incubation. **Panel b, top:** Effect of the strong ferrous chelator bathophenanthroline disulfonate (BPS) on the growth of wild-type cells with either ferric EDTA (20 nM; circles) or FCH (20 nM, squares) as iron source. BPS (100 µM; red symbols) inhibited cell growth when ferric EDTA was the iron source, but not when FCH was the iron source. **Panel b, bottom**: ^{55}Fe uptake from 1 µM FOB (squares) and from 1 µM ferric EDTA (circles) by wild-type cells, in the presence (red) or in the absence (black) of 100 µM of the strong ferrous chelator ferrozine. Ferrozine had no effect on the uptake of FOB, indicating that this siderophore was not reduced prior to uptake by the cells. Data are means ± SD from 4 experiments (biological replicates).

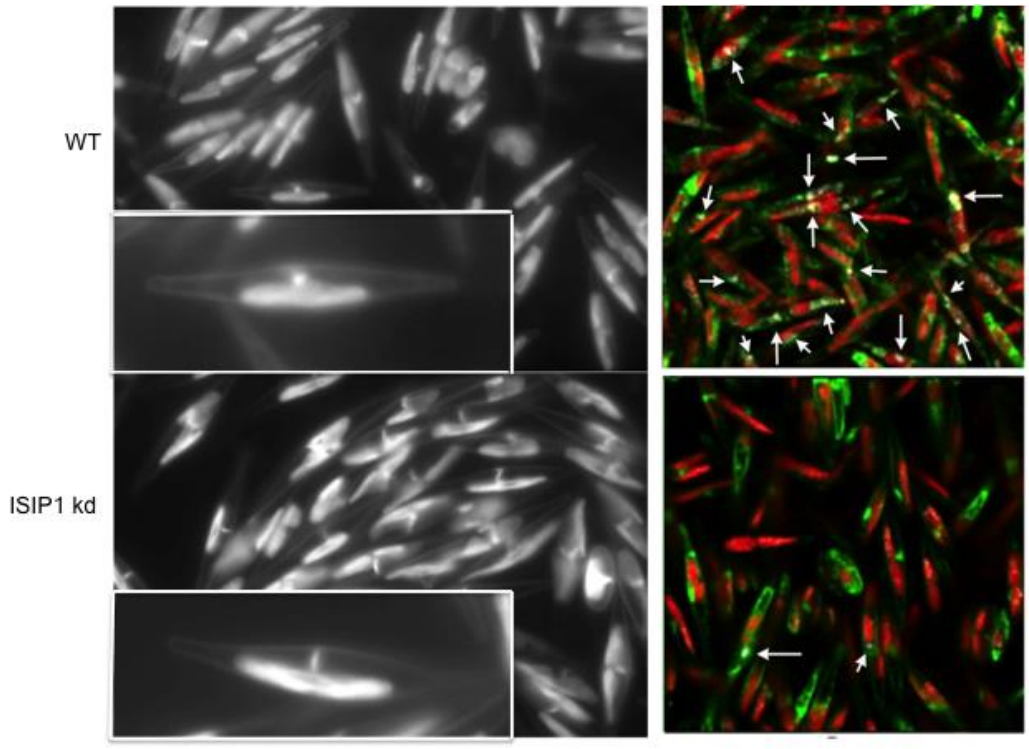

fig. S5. *ISIP1* knockdown lines are defective in endocytosis. Left panels: Wild-type (WT) and *ISIP1* knockdown (ISIP1 kd) cells were grown for one week in iron-deficient medium, harvested and concentrated to about 5 x 10^6 cells/ml, washed twice with iron-free Mf medium, and then resuspended in iron-free Mf medium containing 10 µM of the cell membrane dye FM4-64. After 6 h (20 °C in the dark) the cells were examined by wide-field microscopy. In wild-type cells, a single round-shaped endocytic vesicle originating from the plasma membrane forms near the chloroplast. This vesicle has a different morphology in *ISIP1* knockdown lines. The insets show magnifications of representative single cells. **Right panels:** Confocal scanning laser microscopy of wild-type and *ISIP1* knockdown cells after co-labeling with FM4-64 and the NBD conjugate of FOB (Ga-DFOB-NBD). Wild-type and *ISIP1* knockdown cells were grown for one week in iron-deficient medium, concentrated to about 5 x 10^6 cells/ml and then incubated for 1 h with 10 µM FM4-64. The cells were washed twice with iron-free Mf medium, and then resuspended at 5 x 10^6 cells/ml in iron-free Mf medium containing 1 µM Ga-DFOB-NBD. After 5 h (20 °C in the dark) the cells were harvested by centrifugation, kept on ice, and examined by microscopy (green: FM4-64 fluorescence; red: chlorophyll autofluorescence; white: NBD fluorescence (indicated by arrows)). Note that after 5 h incubation with Ga-DFOB-NBD, the fluorescent siderophore can be detected in several intracellular vesicles, which tend to fuse in a unique peri-chloroplastic vesicle observable after overnight incubation as shown in Fig. 4. In the *ISIP1* knockdown line this vesicle was in general not visible.

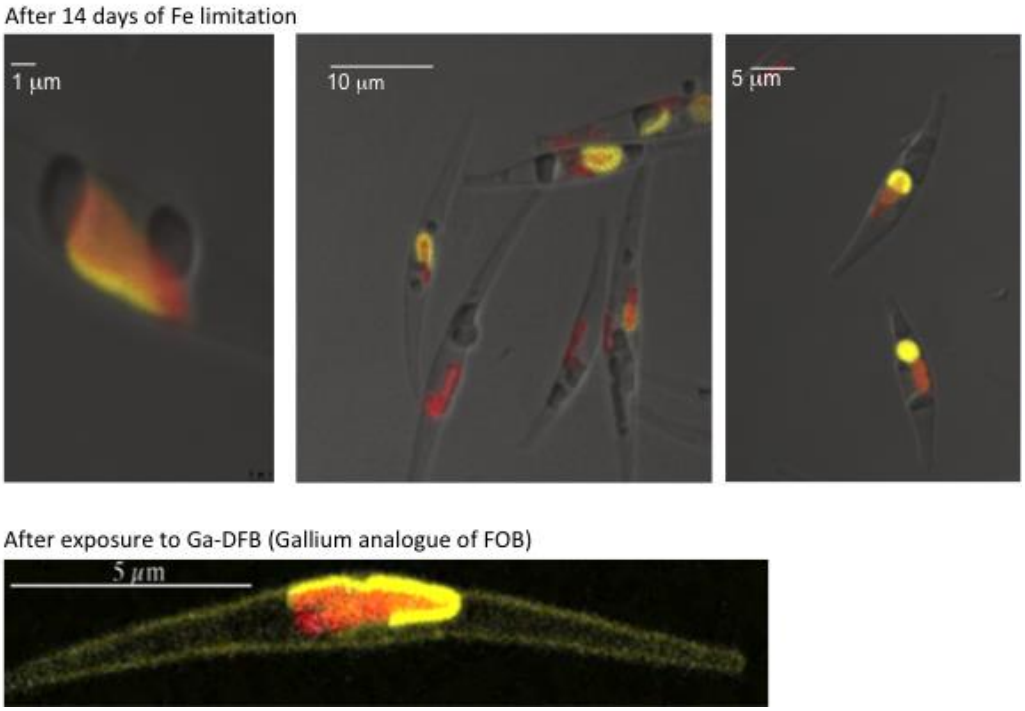

fig. S6. ISIP1-YFP localization and abundance under different Fe supplementation regimes. ISIP1-YFP localizes to the cell surface and the chloroplast membrane in *P. tricornutum*. The top images show cells 14 days after Fe starvation (i.e. incubation in iron-free medium) and bottom images show cells in the early stages of Fe starvation (day 4), stimulated by Ga-FDB, a gallium analogue of FOB. Yellow corresponds to YFP fluorescence, and red corresponds to chlorophyll autofluorescence. Microscopic images were recorded as described in Methods. Scale bars are indicated.

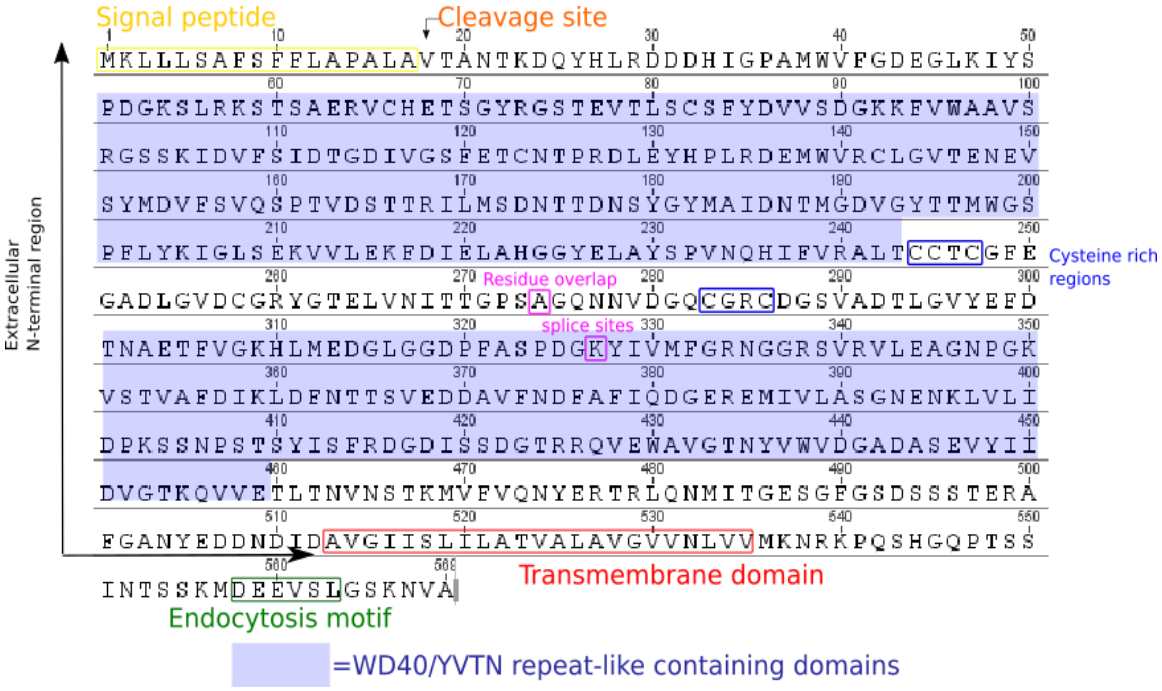

fig. S7. ISIP1 predicted protein sequence and domain features. ISIP1 protein sequence annotation based on bioinformatics analyses. The single C-terminal transmembrance α-helix flanked by hydrophilic regions was predicted by TMNMM (v2.0). The signal peptide and its associated cleavage site were predicted by SignalP (v3.0). The conserved D/EXXL motif (in this case, DEEVSL) was identified at the cytoplasmic tail based on the description of conserved sequences in (*61*). Residue overlap splice sites, and amino acid sequence were obtained from the annotation of the Phatr3 genome (http://ensemblgenomes.org/node/54521). WD40/YVTN repeat-like structural domains were identified by Pfam (v 31.0). The predicted β-propeller folding was confirmed by SWISS-Model.

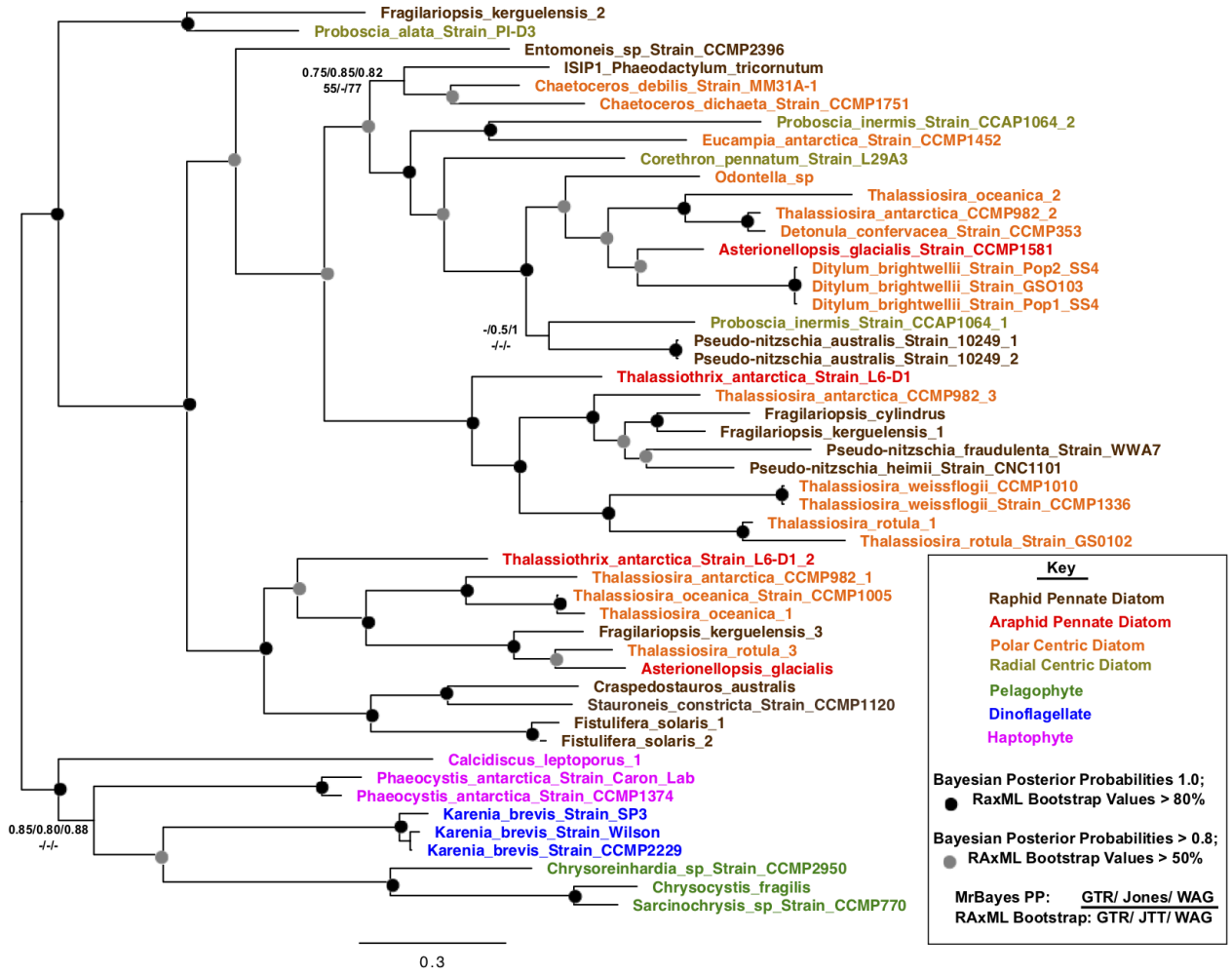

fig. S8. ISIP1 phylogenetic tree. The figure shows a phylogenetic topology for ISIP1. Each branch point was inferred using combined Bayesean and Maximum Likelihood (ML) analysis. Nodes resolved with robust support (posterior probabilities of 1 for three Bayesean inference algorithms and ≥80% bootstrap support for ML) are shown with filled black circles. Where bootstrap support was between 50% and 80% the nodes are in grey. Where support is below these thresholds, individual support values are shown in the following order: top line, Bayesean inferences (GTR, Jones and WAG), bottom line, RAxML (GTR, JTT and WAG).

movie S1. Live cell imaging of the uptake of NBD conjugate of FOB (FOB-NBD) by *P. tricornutum*. FOB-NBD is not fluorescent, while DFOB-NBD is. The cells were grown for 5 days in iron-deficient medium prior to microscopy visualization. The cells were placed directly on slides and visualized immediately after FOB-NBD addition to a final concentration of 1 µM. The confocal images were taken on a Leica TCS SP8 SMD inverted microscope, equipped with pulsed WLL laser, AOBS and two internal spectral SMD-HyD detectors using LAS X software. We used 63x oil immersion objective, 470 nm laser line and detection range for NBD of 500-600 nm and for chlorophyll of 630-681 nm. To suppress cell autofluorescence, which exhibited a very short excited state lifetime, we used for NBD detection 0.3-12 ns time gate. The video was prepared using ImageJ software. Real time scale is indicated within the video as min:sec.